HHS Public Access

Author manuscript

Environ Sci Technol. Author manuscript; available in PMC 2019 November 20.

Published in final edited form as:

Environ Sci Technol. 2018 November 20; 52(22): 12968–12977. doi:10.1021/acs.est.8b04542.

Global and local impacts of delayed mercury mitigation efforts

Hélène Angot[1,*], **Nicholas Hoffman**[2], **Amanda Giang**[1,3], **Colin P. Thackray**[4], **Ashley N. Hendricks**[5], **Noel R. Urban**[5], and **Noelle E. Selin**[1,2]

[1]Institute for Data, Systems, and Society, Massachusetts Institute of Technology, Cambridge, MA 02139, USA.

[2]Department of Earth, Atmospheric, and Planetary Sciences, Massachusetts Institute of Technology, Cambridge, MA 02139, USA.

[3]Institute for Resources, Environment and Sustainability, University of British Columbia, Vancouver, BC Canada V6T 1Z4.

[4]Harvard John A. Paulson School of Engineering and Applied Sciences, Harvard University, Cambridge, MA 02138, USA.

[5]Civil and Environmental Engineering Department, Michigan Technological University, Houghton, MI 49931, USA.

Abstract

Mercury (Hg) is emitted to air by natural and anthropogenic sources, transports and deposits globally, and bioaccumulates to toxic levels in food webs. It is addressed under the global 2017 Minamata Convention, for which periodic effectiveness evaluation is required. Previous analyses have estimated the impact of different regulatory strategies for future mercury deposition. However, analyses using atmospheric models traditionally hold legacy emissions (recycling of previously deposited Hg) constant, and do not account for their possible future growth. Here, using an integrated modeling approach, we investigate how delays in implementing emissions reductions and the associated growing legacy reservoir affect deposition fluxes to ecosystems in different global regions. Assuming nearly constant yearly emissions relative to 2010, each 5-year delay in peak emissions defers by additional extra ca. 4 years the return to year 2010 global deposition. On a global average, each 5-year delay leads to a 14% decrease in policy impacts on local-scale Hg deposition. We also investigate the response of fish contamination in remote lakes to delayed action. We quantify the consequences of delay for limiting the Hg burden of future generations and show that traditional analyses of policy impacts provide best-case estimates.

*angot@mit.edu

SUPPORTING INFORMATION

Results of tests performed to check the robustness of our method and a detailed description of the SERAFM model parameterization are available in Supplementary Information. Additional Tables and Figures are also available: Summary of some characteristics of the modeled lakes (Table S1), Lake geometry values from a lake in Mighigan's Upper Peninsula (Table S2), Ratios of lake characteristics from a lake in Mighigan's Upper Peninsula (Table S3), Lake Hg model evaluation (Fig.S1), Location of Maine and Tribal communities (Fig. S2), Global impact of NP vs. MFR implementation (Fig. S3), Hg emissions in Maine (Fig. S4), Year 2011 U.S. state-level Hg emissions (Fig. S5), Origin of air masses influencing Maine tribal areas (Fig. S6), Total Hg concentration in predatory fish fillets collected in Maine tribal areas (Fig. S7), and Median response of Maine lacustrine predatory fish contamination to delayed implementation of a MFR scenario (Fig. S8).

Graphical Abstract

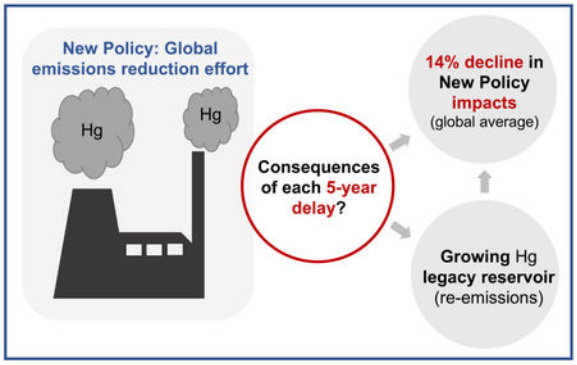

1. INTRODUCTION

Mercury (Hg) is an environmental toxicant dangerous to human health and the environment. Because of its long lifetime in the atmosphere (0.3-1 year)[1,2], Hg travels regionally and globally in its gaseous elemental form (Hg(0)). It deposits to ecosystems by wet and dry processes as Hg(0) and gaseous/particulate divalent Hg (Hg(II)), and converts to highly toxic methylmercury (MeHg) which bioaccumulates in aquatic systems[1,3]. Fish consumption is thus a main source of exposure to Hg for the general population[4–6].

Regulatory actions to reduce human exposure to Hg aim to reduce anthropogenic inputs to the environment. In that context, the Minamata Convention on Mercury[7] entered into force in August 2017 and has 98 parties as of October 2018. Under Article 8, parties “shall take measures to control, and where feasible, reduce emissions of Hg to the atmosphere”, and anthropogenic Hg emissions to the atmosphere are projected to begin to decrease based on current and enhanced policy efforts[8,9]. However, emitted Hg circulates for decades to centuries, and anthropogenic emissions have a long-lasting impact on the global Hg cycle[10]. Legacy emissions (*i.e.,* recycling of previously deposited Hg) from soil and oceanic reservoirs account for about three-fifths of Hg annually emitted to the atmosphere[11]. Even if anthropogenic emissions stay constant, Hg deposition will continue to increase due to legacy emissions[11,12].

Parameterizing legacy emissions in atmospheric models is challenging due to a paucity of models which can capture both three-dimensional atmospheric transport and oceanic/terrestrial cycling simultaneously[13,14]. The majority of policy analyses conducted using atmospheric models therefore only reflect changes in direct anthropogenic emissions, and do not consider the effect of changing legacy emissions. For example, Pacyna et al.[9] estimated that year 2035 global anthropogenic emissions would be reduced by 940 tons compared to 2010 and Hg deposition to ecosystems by 20-30% (except in India) if policy commitments and plans are fully implemented. However, in their analysis, while anthropogenic and natural sources keep emitting Hg during the period 2010-2035 and the Hg legacy reservoir grows, legacy emissions were simulated at 2010 level[9]. Another recent analysis[15] of future policy, investigating projected Hg deposition in Asia by 2050, also did not account for legacy Hg. However, using a biogeochemical cycle model, the authors estimated that legacy Hg changes

could alter the magnitude of calculated policy impacts by 30%, but they did not resolve this effect spatially.

Here, using an integrated approach that combines biogeochemical cycle modeling with global-scale chemical transport modeling, we investigate the impacts of delayed global action on global- and local-scale Hg deposition and evaluate associated changes in policy impacts, including their spatial resolution. We test the hypothesis that a longer delay in near-term peak emissions will lead to a larger Hg legacy pool and thus a measurable influence on expected policy impacts. We further examine consequences of delayed global mitigation efforts in different regions of the world to illustrate implications relevant to environmental justice concerns. For one of these regions, a Native American community in the U.S., we examine the impact on fish contamination in remote lakes where the main source of contamination is atmospheric deposition from the global Hg pool.

2. METHODS

2.1 Conceptual framework

The conceptual framework of this study is presented in Fig. 1. Present-day (2010) and future simulations were performed using the chemical transport model (CTM) GEOS-Chem (see Section 2.3). As in traditional future projections with other atmospheric models[9], legacy emissions were initially assumed constant to 2010 level to calculate the effects of changes in direct anthropogenic emissions (see Section 2.2). A global biogeochemical cycle (GBC) model was used to calculate a global legacy penalty as a function of the amount of emission since 2010 (see Section 2.4). This global legacy penalty was then spatially-distributed and added to future deposition fluxes from the CTM (see Section 2.4). Using this approach, adjusted Hg deposition from the CTM and the effective policy impacts differ as a function of the total amount of mercury emitted, which is greater for longer policy delay. Adjusted Hg deposition fluxes were then used as inputs to a lake Hg model (see Section 2.5) to investigate the influence of delayed global action on lacustrine fish contamination.

Throughout this paper, we compare policy impacts assuming an immediate (*i.e.,* traditional method – no delay/legacy penalty) or delayed global action to reduce emissions. For each grid box of the CTM, policy impacts (PI, in $\Delta\mu g/m^2/yr$) are calculated as the difference in total deposition between future and present-day simulations. The percent change (PC) in policy impacts due to a global action delayed to year YYYY (YYYY = 2020, 2025, 2030, 2035, or 2050) is calculated according to Equation (1):

$$PC_{YYYY} = \frac{PI_{action\ delayed\ to\ YYYY} - PI_{traditional\ method}}{PI_{traditional\ method}} \times 100\,. \quad (1)$$

The mean percent change in policy impacts, given by Equation (2), is the average percent change due to a near-term (2020-2035) 5-year delay:

$$\overline{PC} = \frac{(PC_{2035} - PC_{2030}) + (PC_{2030} - PC_{2025}) + (PC_{2025} - PC_{2020})}{3}. \quad (2)$$

2.2 Present-day and future emissions scenarios

Simulations performed with the CTM and the GBC model are listed in Table 1. The GEOS-Chem present-day (2010) BASE simulation was performed using the AMAP/UNEP inventory[17], applying emission controls to U.S., Canadian, European and Chinese emissions from coal fired power plants[18]. The CTM PRE-2010 LEGACY simulation was performed to quantify deposition from current (2010) legacy emissions and evaluate its spatial pattern. FUTURE simulations were performed using gridded emissions inventories developed by Pacyna et al.[9]. Briefly, the Current Policy (CP) scenario projects that annual Hg emissions will slightly increase in 2035 (ca. +75 Mg compared to 2010, *i.e.,* +3.02 Mg yr^{-1}). Increasing energy demand contributing to increased emissions globally will be offset by the implementation of additional control measures. The more stringent New Policy (NP) scenario indicates that annual emissions will significantly decrease by 2035 (ca. −820 Mg compared to 2010, *i.e.,* −32.7 Mg yr^{-1}). This scenario assumes that policy commitments and plans announced by countries worldwide to reduce greenhouse gas emissions and phase out fossil fuel subsidies are fully implemented. Additionally, this scenario assumes that the use of Hg in products will be reduced by 70% by implementing Article 4 of the Minamata Convention on Hg-added products. Finally, the Maximum Feasible Reduction (MFR) scenario leads to a dramatic decrease of annual Hg anthropogenic emissions (ca. −1500 Mg compared to 2010, *i.e.,* −59.9 Mg yr^{-1}). In this scenario, all countries reach the highest feasible reduction efficiency in each emission sector.

The GBC model was driven by 2000 BCE to 2008 CE primary anthropogenic emissions from Streets et al.[19], Hg discharges from rivers (held constant at present-day levels)[16], and global geogenic emissions (90 Mg yr^{-1})[20,21]. For consistency with the emissions inventories used in the CTM, we did not include additional 1850-2008 atmospheric Hg emissions from commercial products (105 Gg) proposed by Horowitz et al.[22]. For 2009-onward primary anthropogenic emissions, we used future emissions scenarios developed by Pacyna et al.[9] as described above.

2.3 Chemical transport modeling

The global CTM GEOS-Chem (www.geos-chem.org) was used to project present-day and future total (wet+dry) gross Hg deposition fluxes to ecosystems. The model is driven by assimilated meteorological data from the NASA GMAO Goddard Earth Observing System[23]. MERRA-2 data were used for the simulations (https://gmao.gsfc.nasa.gov/products/). GEOS-Chem is a global-scale model that couples a 3D atmosphere[2,24,25], a 2D surface-slab ocean[26], and a 2D terrestrial reservoir[27] at a 2°×2.5° horizontal resolution. A two-step oxidation mechanism of Hg(0) initiated by Br was used. The second-stage HgBr oxidation is mainly by the NO_2 and HO_2 radicals using the new mechanism for atmospheric redox chemistry developed by Horowitz et al.[2]. Oxidant fields from Schmidt et al.[28] have 4°×5° horizontal resolution. Photoreduction of aqueous-phase Hg(II)-organic complexes is

dependent on the local concentration of organic aerosols, the NO_2 photolysis frequency, and an adjusted coefficient (K_RED_JNO2) set to 9.828×10'^{2} m^3 μg^{-1} here for simulations with MERRA-2 meteorological fields and use of the slab ocean[29]. For further details, a comprehensive description of the model is available elsewhere[30].

2.4 Legacy penalty

We used a previously-published fully coupled seven-reservoir GBC model[11,16] (available at https://github.com/SunderlandLab/gbc-boxmodel) to scale legacy emissions. The model allows full coupling of the atmosphere, ocean (surface, subsurface, and deep ocean), and terrestrial ecosystems (fast terrestrial, slow and armored soils). Hg cycles between reservoirs and is ultimately removed by burial in deep marine sediments. In order to evaluate the impact of delayed action on global Hg deposition, incremental 5-year delays in implementing a NP or MFR scenario were tested (see Table 1, FUTURE simulations). We assumed a CP scenario (*i.e.,* a 3.02 Mg yr^{-1} increase) until implementation of a NP or MFR scenario. A total of six simulations were performed with the GBC model (PRE-2010 and PRE-YYYY LEGACY in Table 1) in order to quantify the contribution to global Hg deposition of emissions during the policy delay Δt. The Δt-dependent global legacy penalty was defined as the difference in global deposition between PRE-YYYY and PRE-2010 LEGACY simulations (where YYYY = 2020, 2025, 2030, 2035, or 2050). The global legacy penalty was then spatially-distributed (see below) and added to future deposition fluxes from the CTM in each grid-box (see Fig. 1). Rather than assuming a globally homogeneous distribution of legacy emissions (*i.e.,* global legacy penalty evenly divided among all 2°×2.5° grid boxes of the CTM), we used the spatial distribution of the legacy emissions contribution to Hg deposition (PRE-2010 LEGACY simulation with the CTM, see Table 1). Spatial differences in legacy impact relate to atmospheric transport, geographic factors (e.g., land *vs.* ocean) and reemissions. In GEOS-Chem, reemission of Hg previously deposited to land follows the deposition patterns of current sources[31].

Local consequences of delayed global action for Hg deposition fluxes to ecosystems are discussed (see Section 3.2) at four selected sites located at varying distance from anthropogenic sources: A) tribal areas of Eastern Maine, USA, representative of remote regions and used to illustrate implications relevant to environmental justice concerns (see Section 3.3); B) Ahmedabad, the largest city of the Indian state of Gujarat and the location of two coal-fired power plants of more than 1000 MW electricity generation[32]; C) Shanghai, China's biggest city and one of the main industrial centers, where elevated atmospheric Hg concentrations have been reported[33–35]; and D) an area of the Southern Pacific known for albacore tuna fisheries[36]. Sunderland et al.[37] recently estimated that seafood harvested from the Equatorial and South Pacific Ocean accounts for 25% of the U.S. population-wide MeHg intake.

2.5 Fish contamination

To investigate the influence of delayed global action on fish contamination, we used a recently-developed implementation of the mechanistic model SERAFM (Spreadsheet-based Ecological Risk Assessment for the Fate of Mercury) of Hg in aquatic environments developed by the U.S. Environmental Protection Agency (EPA)[38,39]. This model has been

widely used and evaluated since its development[40–46]. The implementation of SERAFM used here was developed by Hendricks[47] in the programming language R and modified for non-steady state conditions to enable prediction of lake responses to changes in loadings. A description of this mass balance model is provided by Perlinger et al.[48]. Briefly, the model is a three-reservoir box model (epilimnion, hypolimnion, and sediments). It enables prediction of aqueous Hg concentrations based on the characteristics of the lake of interest (*e.g.,* depth, retention time), its watershed (*e.g.,* surface area), and the local Hg atmospheric deposition flux. The model does not include fish population dynamics and solves for an annually averaged MeHg concentration in the water column that is multiplied by bioaccumulation factors (BAFs) for mixed feeders or piscivorous fish[38] to give a distribution of MeHg concentrations in fish. We therefore neglect the time required (3-7 years) for fish populations to reach steady state following a change in Hg loadings[48–50]. Additionally, Hg runoff from catchments is set to be proportional to atmospheric deposition (see S.I. Section 1.2.a). This approach assumes that only recently deposited Hg is susceptible to leaching leading to a fast response to changes in Hg deposition[48]. More information regarding the parameterization used here and the model performance can be found in S.I. Section 1.2 and Fig.S1.

Although some lake Hg contamination can be attributed to direct inputs from local sources[51, 52], we focus here on remote lakes where the main source of contamination is atmospheric deposition from the global Hg pool (see Section 3.2). More specifically, we concentrate on remote tribal regions of Eastern Maine, USA (see Fig.S2) since Native Americans are particularly vulnerable to Hg contamination due to traditional subsistence fishing[53]. In order to investigate the response to changes in atmospheric deposition, the model was first run for 10 years (2000-2010) to reach steady-state, and then transiently using the adjusted deposition values from the CTM described in Section 2.1. Here, we evaluated the response of fish contamination to delayed global action assuming everything else (*e.g.*, food web structure, nutrient loading) constant. While Hg biogeochemical cycling will be affected by climate and land-use change[14,54–56], this is not taken into account here for consistency and ease of comparison with other traditional policy impact studies.

3. RESULTS AND DISCUSSION

3.1 Impact of delayed action on global Hg deposition

The impact of delayed action on global Hg deposition was quantified using the fully coupled seven-reservoir GBC model[11,16] (FUTURE simulations, see Table 1). Fig.2a shows global anthropogenic emissions to the atmosphere from 1950 onward. Emissions rise steadily after 1950 due to increased coal use and artisanal gold mining[19]. Over recent years, decreasing emissions in Europe and North America due to domestic regulation have been offset by an increase in East Asia, leading to an overall increase[9,19]. Global Hg deposition is depicted in Fig.2b. The atmosphere responds relatively quickly (though not proportionally) to decreasing emissions. If a NP scenario is implemented in 2020, deposition begins to decrease by 2021. In this scenario, global primary emissions decrease by ca. 980 Mg from 2020 to 2050 while deposition decreases by ca. 635 Mg. These results reflect the balance and cycling of Hg between the various reservoirs. Return to year 2010 deposition (arbitrary threshold) is achieved in 2038, *i.e.,* 18 years after NP implementation. On the other hand,

return to year 2010 deposition is achieved in 2027 if a more stringent MFR scenario is implemented in 2020 (see Fig.S3).

To evaluate the impact of delayed global action, a NP scenario was implemented for various years between 2020 and 2050. Return to year 2010 deposition level is reached in 2038, 2047, 2056, or 2064 if a NP scenario is implemented in 2020, 2025, 2030, or 2035, respectively. On average, each near-term 5-year delay in implementing a NP scenario in turns delays by additional extra ca. 4 years a return to its year 2010 level (this level is not the goal of policy action but used here for illustrative purposes). Each near-term 5-year delay leads to a ca. 2.2% increase of the atmospheric reservoir mass, mainly due to the feedback from legacy emissions.

Based on these results, we also compare the emissions reduction rate needed in order to reach the same given deposition target at the same time but assuming delayed global action. According to Fig.2b, return to year 2010 deposition level is reached in 2038 if emissions reduction is initiated in 2020 at a −32.7 Mg yr^{-1} reduction rate (NP). To reach the same deposition target (year 2010 level) at the same time (2038), reduction rates of −48.0, −83.0 and −230.0 Mg yr^{-1} are needed if emissions reduction is initiated in 2025, 2030, or 2035, respectively. In other words, emissions reduction must be ca. 1.5, 2.5 or 7.0 times more stringent if initiated in 2025, 2030 or 2035, respectively, instead of 2020 due to legacy emissions and increasingly shortened recovery periods.

3.2 Local consequences and percent change in policy impacts

Using the integrated modeling approach described in Section 2.1, we calculated the local consequences of delayed global action for Hg deposition fluxes to ecosystems at the four selected sites (see Section 2.4). Following a traditional atmospheric modeling method (*i.e.,* no delay/legacy penalty – see Fig. 1), the NP scenario leads to a 15.3%, 55.1%, and 12.9% decrease in Hg deposition (*vs.* present-day levels) in Maine, Shanghai, and the South Pacific, respectively (see Table 2). In contrast, a 25.9% increase is observed in Ahmedabad, India due to projected growth of regional anthropogenic emissions[9]. The MFR scenario leads to consistent global-scale Hg deposition reduction, with a 25.8%, 38.4%, 68.3%, and 22.1% decrease in Maine, Ahmedabad, Shanghai, and the South Pacific, respectively. These results are consistent with those reported by Pacyna et al.[9] despite the use of the a different CTM with a formulation, spatial resolution, and physical and chemical process parameterizations considerably different from GLEMOS and ECHMERIT[30].

As expected, policy impacts are lower in remote regions, far from emissions sources[9,48, 57]. While North America contributes a significant fraction of global anthropogenic emissions[17,58,59], Hg emissions are low in Maine[60] (~50 kg yr^{-1}) and in the neighboring New England states (see Fig.S4 and Fig.S5) due to a lack of major emitting sources as well as the adoption in 1998 of a regional Hg action plan with aggressive emission reduction goals[61]. Based on Fig. 1 in Giang and Selin[57], little impact is expected from domestic U.S. regulations in eastern Maine in terms of avoided deposition. As inferred by 2007-2016 hourly air back-trajectories computed with the HYSPLIT model[62] (see Fig.S6), Maine tribal areas are mainly influenced by air masses originating from Canada and the Arctic (Hudson Bay), *i.e.,* the Northern Hemisphere atmospheric background, rather than U.S. emissions.

Sunderland et al.[63] also showed that, in the early 2000s, anthropogenic emissions in the U.S. and Canada resulted in ~30% of Hg deposition to the Gulf of Maine, with the rest (~ 70%) from global anthropogenic and natural sources. In that context, a decrease of Hg deposition in Maine tribal areas can only be achieved through the reduction of the global background Hg concentration, *i.e.,* through global action. Potential additional effects of global change (climate, biomass burning, land use) on Hg deposition have recently been investigated in Michigan's Upper Peninsula (USA) and projected to have modest impacts compared to changes in direct anthropogenic emissions[48].

Figure 3 depicts the mean percent change in policy impacts due to a near-term (2020-2035) 5-year delayed implementation of a NP scenario. On a global average, each 5-year delay leads to a ca. 14% decrease in NP impacts. The consequences of delayed global action depend on the stringency of the policy as each 5-year delay leads to a ca. 8% decrease in MFR impacts (global average, see Table 2). Remote regions are proportionally more impacted by delayed global action than regions close to emission sources and a clear gradient between the Northern and Southern Hemispheres can be observed (see Fig.3). While a 5-year delay leads to a −12.5 and −16.2% change in NP impacts in Maine and South Pacific, respectively, it induces a −5.4 and −1.1% change in Ahmedabad and Shanghai, respectively (see Table 2 and Fig.3). This can be explained by the relatively lower policy impact in remote regions (see above) and therefore proportionally higher influence of the legacy penalty. Consequences in terms of human exposure through fish consumption are further discussed in the next section, with a specific focus on remote inland waters of Eastern Maine, USA.

3.3 Local impacts on fish contamination: a tribal case study

In the U.S., rates of fish consumption and type of fish consumed vary widely. Whereas fish forms a small component of the diet of many Americans, some groups such as Native American tribes eat fish as frequently as daily[65–67]. Additionally, fishing is an important component of cultural and religious practice for many Native Americans[68]. Therefore, fish contamination poses special risks for tribal members and is an issue relevant to environmental justice[68]. According to a study performed in Maine tribal areas[69], total Hg concentration in predatory fish exceeds the 0.3 mg kg^{-1} U.S. EPA threshold[70] in 16 out of 20 lakes (see Fig.S7) despite their remoteness from emissions sources (see Section 3.2). As discussed by Perlinger et al.[48], the susceptibility of lakes to being contaminated depends on the total supply of Hg to lakes but more importantly on factors leading to production and accumulation of MeHg (*e.g.*, prevalence of forests and wetlands in the catchment, low alkalinity, pH or nutrients, and long water residence time). In order to navigate the gap between safe and desired fish consumption levels for populations with significant exposure to Hg, it is necessary to model changes in fish contamination over time[71] and to investigate the response to delayed global action.

The median response (over 20 lakes, see S.I. Section 1.2) of lacustrine predatory fish contamination to changes in atmospheric deposition can be seen in Fig.4. All the lakes within the study area respond with a rapid decrease in MeHg concentration over a decade, followed by a slower decline toward steady state. Using the SERAFM model, Knightes et al.

[39] modeled the response to a hypothetical 50% decline in deposition across a range of lake types and also found a similar response. However, the time response reported here is at the upper range of those reported in Knightes et al.[39]. Assuming an immediate implementation of a NP scenario (*i.e.,* no delay/legacy penalty – traditional method), the median MeHg concentration in predatory fish rapidly declines by ca. 11%. This suggests that even in the case of an immediate NP implementation and of a rather fast response time to changes in deposition, the median MeHg concentration is still above the U.S. EPA threshold. These results are in line with those recently reported in Michigan's Upper Peninsula[48]. Substantial and rapid response of fish contamination to reduced emissions have been observed near emissions sources[72–74]. However, the relatively lower policy impacts in remote areas (see Section 3.2) are likely to considerably prolong the time required to see substantial decreases in fish Hg concentrations. Under an immediate implementation of a MFR scenario, the median MeHg concentration drops to about 0.3 mg kg^{-1}, *i.e.,* the U.S. EPA threshold. A desired subsistence fish consumption of 300-500 grams per day requires a safe level target of ~0.018 mg kg^{-1} [48,66,71]. The predatory fish Hg concentrations under the MFR scenario therefore indicate that, even under the strictest global Hg regulations, a traditional-subsistence diet high in predatory fishes (*e.g.,* brook trout, brown trout, burbot, landlocked salmon, smallmouth bass) will lead to unsafe MeHg exposure in Maine tribal areas. While flawed from the standpoint of environmental justice, a diet that shifts toward mixed feeders (*e.g* white sucker, also known as mullet or bay fish) would reduce MeHg exposure (see Fig.S1). This suggestion also holds true for riverine fish in the study area[75]. Although not a true substitute for a pristine environment, another alternative is the increasing consumption of lower-Hg containing fish from aquaculture[55]. The Aroostook Band of Micmacs located in Presque Isle (see Fig.S2) has recently made this choice and created a recirculating aquaculture brook trout fish hatchery[76].

The impact of delayed global action on MeHg fish concentrations was then evaluated. Return to year 2010 MeHg level (an arbitrarily-defined threshold used here for illustrative purposes) is achieved in 2021, 2027, 2033, or 2043 if a NP scenario is implemented in 2020, 2025, 2030, or 2035, respectively. In other words, the longer the delay, the longer it takes to reach the same MeHg concentration target. While the U.S. EPA threshold is reached in a decade if a MFR scenario is implemented in 2010 (see Fig.4), this target is never reached in case of delayed MFR implementation (see Fig.S8).

3.4 Uncertainties in atmospheric Hg modeling

Uncertainties in atmospheric Hg modeling for policy evaluation, in particular for linking sources to receptors, have recently been thoroughly discussed by Kwon and Selin[13]. Major uncertainties arise from biogeochemical cycling, atmospheric chemistry, and anthropogenic emissions. There is for example ongoing controversy in the literature and a rapidly evolving understanding of Hg pool sizes and fluxes in the global Hg cycle [13,22,77–81]. The fully coupled seven-reservoir GBC model[11,16] used in this study to scale legacy emissions is based on Streets et al.'s[19] all-time emission inventory, which assumes a major atmospheric Hg impact from late 19th century Gold Rush mining in North America. Recent studies, including historical documents on Hg use, ore geochemistry and a large array of ice and lake sediment records, have challenged this account, as documented in a critical review by

Outridge et al.[77]. This synthesis argues for a “low-mining emissions” scenario which translates into smaller legacy pools in the oceans and soils than considered until now. In order to investigate the consequences of a smaller legacy pool on the calculated legacy penalty, we cut historical (1850-1920 CE) mining emissions in the Streets et al.[19] inventory by 50%, as proposed by Engstrom et al.[78]. This “low-mining emissions” scenario did not lead to any significant change in the influence of delayed action on NP policy impacts. As suggested by Amos et al.[79], atmospheric deposition is most sensitive to the profile of anthropogenic emissions in recent decades, and results presented here are robust to the uncertainty in historical emissions. Our results also depend on the emissions scenario used from year 2010 until implementation of the NP scenario. We conducted a perturbation analysis to investigate the effect of this uncertainty on the percent change in policy impact. We calculated a mean legacy penalty for each near-term 5-year delay of 107 Mg, 115 Mg (see Table 2), or 123 Mg assuming constant emissions (+ 0 Mg yr^{-1}), a CP scenario (+3.02 Mg yr^{-1}), or a 2×CP (+6.04 Mg yr^{-1}) rate. We find that, on a global average, each 5-year delay leads to a 13%, 14% or 15% decrease in NP policy impacts, respectively. Perturbations to the legacy penalty therefore have little impact on our results.

3.5 Implications

Our results show that traditional spatially-resolved analyses of prospective policy impacts from mercury reductions that do not consider future changes in legacy emissions can overestimate changes driven by policy implementation by up to 110% by 2050 and should be considered as best-case estimates. Though legacy impacts have previously been evaluated at global scale using global biogeochemical cycling models, these effects are not widely appreciated by policy-makers. Selin[12] recently proposed a global metric to help policy-makers better understand the implications of policy options by taking into account near-term changes in legacy Hg. Using the integrated modeling approach described here, the effect of legacy Hg changes on policy impact can be resolved spatially. Future work could build upon this study by (re)examining the impact of other or upcoming future emission scenarios beyond those developed by Pacyna et al.[9] evaluated here. Future policy analyses should account for future legacy emissions and associated deposition to better inform policy decision-making; the approach outlined here provides a straightforward methodology to estimate this effect without relying on advanced coupled atmosphere-ocean models. Alternately, an even simpler approach could scale legacy emissions and resulting deposition globally using a global-scale estimate of biogeochemical model output[12] if running a global biogeochemical cycle is infeasible.

Our results highlight the benefits of near-term aggressive Hg mitigation efforts. Return to year 2010 global deposition is achieved 2.6 times faster under a MFR vs. NP scenario (see Section 3.1). Contrary to the NP scenario, the MFR scenario leads to consistent global-scale Hg deposition reduction (see Section 3.2). We also show that each near-term delay in taking global action to reduce emissions has a non-negligible influence on expected policy impacts due to legacy emissions. Global emissions reduction must be ca. 1.5, 2.5 or 7.0 times more stringent if initiated in 2025, 2030 or 2035, respectively, instead of 2020 (see Section 3.1). On a global average, each 5-year delay leads to a ca. 14% decrease in NP impacts (see Section 3.2). Finally, while the median MeHg concentration in predatory fish in Maine lakes

is still ca. 25% too high for safe fish consumption in case of an immediate NP implementation, the U.S. EPA threshold is achieved under immediate implementation of a MFR scenario (see Section 3.3). However, this level is never reached if policy is delayed. It should also be emphasized that under a business-as-usual scenario (CP), deposition fluxes to ecosystems will gradually increase. Even if moderately delayed, NP and MFR scenarios lead to reductions in Hg deposition and MeHg concentration, highlighting the positive impact of concerted global action.

Supplementary Material

Refer to Web version on PubMed Central for supplementary material.

ACKNOWLEDGMENTS

This work was supported by the MIT Leading Technology & Policy Program, a core center grant P30-ES002109 from the National Institute of Environmental Health Sciences – National Institute of Health, the MIT EAPS Undergraduate Research Opportunities Program, and the National Institute of Environmental Health Sciences Superfund Basic Research Program – National Institute of Health (P42 ES027707). The authors would like to thank J. Pacyna and S. Cinnirella for providing future emissions inventories. HA would like to acknowledge F. Corey, D. Macek, S. Venno, A. Ajmani, B. Longfellow, C. Johnson, N. Dalrymple, and K. M. Vandiver for rewarding discussions during field trips to Maine.

REFERENCES

(1). Selin NE Global Biogeochemical Cycling of Mercury: A Review. Annual Review of Environment and Resources 2009, 34 (1), 43–63.

(2). Horowitz HM; Jacob DJ; Zhang Y; Dibble TS; Slemr F; Amos HM; Schmidt JA; Corbitt ES; Marais EA; Sunderland EM A New Mechanism for Atmospheric Mercury Redox Chemistry: Implications for the Global Mercury Budget. Atmos. Chem. Phys 2017, 17 (10), 6353–6371.

(3). Gustin MS; Lindberg SE; Weisberg PJ An Update on the Natural Sources and Sinks of Atmospheric Mercury. Applied Geochemistry 2008, 23, 482–493.

(4). Mergler D; Anderson HA; Chan LHM; Mahaffey KR; Murray M; Sakamoto M; Stern AH Methylmercury Exposure and Health Effects in Humans: A Worldwide Concern. AMBIO: A Journal of the Human Environment 2007, 36 (1), 3–11.

(5). Du B; Feng X; Li P; Yin R; Yu B; Sonke JE; Guinot B; Anderson CWN; Maurice L Use of Mercury Isotopes to Quantify Mercury Exposure Sources in Inland Populations, China. Environ. Sci. Technol 2018, 52 (9), 5407–5416. [PubMed: 29649864]

(6). Sunderland EM Mercury Exposure from Domestic and Imported Estuarine and Marine Fish in the U.S. Seafood Market. Environ Health Perspect 2007, 115 (2), 235–242. [PubMed: 17384771]

(7). UNEP. Text of the Minamata Convention on Mercury, Available at: Http://Mercuryconvention.Org/Portals/11/Documents/Booklets/COP1%20version/Minamata-Convention-Booklet-Eng-Full.Pdf, Last Access: 18 April 2018 2017.

(8). Ancora MP; Zhang L; Wang S; Schreifels JJ; Hao J Meeting Minamata: Cost-Effective Compliance Options for Atmospheric Mercury Control in Chinese Coal-Fired Power Plants. Energy Policy 2016, 88 (C), 485–494.

(9). Pacyna JM; Travnikov O; De Simone F; Hedgecock IM; Sundseth K; Pacyna EG; Steenhuisen F; Pirrone N; Munthe J; Kindbom K Current and Future Levels of Mercury Atmospheric Pollution on a Global Scale. Atmos. Chem. Phys 2016, 16 (19), 12495–12511.

(10). Selin Noelle E Global Change and Mercury Cycling: Challenges for Implementing a Global Mercury Treaty. Environmental Toxicology and Chemistry 2014, 33 (6), 1202–1210. [PubMed: 24038450]

(11). Amos HM; Jacob DJ; Streets DG; Sunderland EM Legacy Impacts of All-Time Anthropogenic Emissions on the Global Mercury Cycle. Global Biogeochem. Cycles 2013, 27 (2), 410–421.

(12). Selin NE A Proposed Global Metric to Aid Mercury Pollution Policy. Science 2018, 360 (6389), 607–609. [PubMed: 29748274]

(13). Kwon SY; Selin NE Uncertainties in Atmospheric Mercury Modeling for Policy Evaluation. Curr Pollution Rep 2016, 2 (2), 103–114.

(14). Obrist D; Kirk JL; Zhang L; Sunderland EM; Jiskra M; Selin NE A Review of Global Environmental Mercury Processes in Response to Human and Natural Perturbations: Changes of Emissions, Climate, and Land Use. Ambio 2018, 47 (2), 116–140. [PubMed: 29388126]

(15). Giang A; Stokes LC; Streets DG; Corbitt ES; Selin NE Impacts of the Minamata Convention on Mercury Emissions and Global Deposition from Coal-Fired Power Generation in Asia. Environ. Sci. Technol 2015, 49 (9), 5326–5335. [PubMed: 25851589]

(16). Amos HM; Jacob DJ; Kocman D; Horowitz HM; Zhang Y; Dutkiewicz S; Horvat M; Corbitt ES; Krabbenhoft DP; Sunderland EM Global Biogeochemical Implications of Mercury Discharges from Rivers and Sediment Burial. Environ. Sci. Technol 2014, 48 (16), 9514–9522. [PubMed: 25066365]

(17). AMAP/UNEP. Technical Background Report for the Global Mercury Assessment 2013.; Arctic Monitoring and Assessment Porgramme, Oslo, Norway. UNEP Chemicals Branch, Geneva, Switzerland, 2013; p 263.

(18). Zhang Y; Jacob DJ; Horowitz HM; Chen L; Amos HM; Krabbenhoft DP; Slemr F; Louis VLS; Sunderland EM Observed Decrease in Atmospheric Mercury Explained by Global Decline in Anthropogenic Emissions. PNAS 2016, 113 (3), 526–531. [PubMed: 26729866]

(19). Streets DG; Devane MK; Lu Z; Bond TC; Sunderland EM; Jacob DJ All-Time Releases of Mercury to the Atmosphere from Human Activities. Environ. Sci. Technol 2011, 45 (24), 10485–10491. [PubMed: 22070723]

(20). Pirrone N; Cinnirella S; Feng X; Finkelman R; Friedli H; Leaner J; Mason R; Mukherjee A; Stracher G; Streets D; Telmer K Global Mercury Emissions to the Atmosphere from Anthropogenic and Natural Sources. Atmospheric Chemistry and Physics 2010, 10, 5951–5964.

(21). Bagnato E; Aiuppa A; Parello F; Allard P; Shinohara H; Liuzzo M; Giudice G New Clues on the Contribution of Earth's Volcanism to the Global Mercury Cycle. Bull Volcanol 2011, 73 (5), 497–510.

(22). Horowitz HM; Jacob DJ; Amos HM; Streets DG; Sunderland EM Historical Mercury Releases from Commercial Products: Global Environmental Implications. Environ. Sci. Technol 2014, 48 (17), 10242–10250. [PubMed: 25127072]

(23). Bey I; Jacob DJ; Yantosca RM; Logan JA; Field BD; Fiore AM; li Q; Liu HY; Mickley LJ; Schultz MG Global Modeling of Tropospheric Chemistry with Assimilated Meteorology: Model Description and Evaluation. Journal of geophysical research 2001, 106 (D19), 23,073–23,095.

(24). Holmes CD; Jacob DJ; Corbitt ES; Mao J; Yang X; Talbot R; Slemr F Global Atmospheric Model for Mercury Including Oxidation by Bromine Atoms. Atmospheric Chemistry and Physics 2010, 10, 12037–12057.

(25). Amos HM; Jacob DJ; Holmes CD; Fisher JA; Wang Q; Yantosca RM; Corbitt ES; Galarneau E; Rutter AP; Gustin MS; Steffen A; Schauer JJ; Graydon JA; Louis VL; Talbot RW; Edgerton ES; Zhang Y; Sunderland EM Gas-Particle Partitioning of Atmospheric Hg(II) and Its Effect on Global Mercury Deposition. Atmos. Chem. Phys 2012, 12 (1), 591–603.

(26). Soerensen AL; Sunderland EM; Holmes CD; Jacob DJ; Yantosca RM; Skov H; Christensen JH; Strode SA; Mason RP An Improved Global Model for Air-Sea Exchange of Mercury: High Concentrations over the North Atlantic. Environ. Sci. Technol 2010, 44 (22), 8574–8580. [PubMed: 20973542]

(27). Selin NE; Jacob DJ; Yantosca RM; Strode S; Jaeglé L; Sunderland EM Global 3-D Land-Ocean-Atmosphere Model for Mercury: Present-Day versus Preindustrial Cycles and Anthropogenic Enrichment Factors for Deposition. Global Biogeochem. Cycles 2008, 22 (2), GB2011.

(28). Schmidt JA; Jacob DJ; Horowitz HM; Hu L; Sherwen T; Evans MJ; Liang Q; Suleiman RM; Oram DE; Le Breton M; Percival CJ; Wang S; Dix B; Volkamer R Modeling the Observed Tropospheric BrO Background: Importance of Multiphase Chemistry and Implications for Ozone, OH, and Mercury. J. Geophys. Res. Atmos 2016, 121 (19), 2015JD024229.

(29). Hg and POPs working group. GEOS-Chem mercury simulations http://wiki.seas.harvard.edu/geos-chem/index.php/Mercury#K_RED_JNO2 (accessed May 15, 2018).

(30). Travnikov O; Angot H; Artaxo P; Bencardino M; Bieser J; D'Amore F; Dastoor A; De Simone F; Diéguez MDC; Dommergue A; Ebinghaus R; Feng XB; Gencarelli CN; Hedgecock IM; Magand O; Martin L; Matthias V; Mashyanov N; Pirrone N; Ramachandran R; Read KA; Ryjkov A; Selin NE; Sena F; Song S; Sprovieri F; Wip D; Wangberg I; Yang X Multi-Model Study of Mercury Dispersion in the Atmosphere: Atmospheric Processes and Model Evaluation. Atmos. Chem. Phys 2017, 17 (8), 5271–5295.

(31). Selin NE; Jacob DJ; Park RJ; Yantosca RM; Strode S; Jaeglé L; Jaffe DA Chemical Cycling and Deposition of Atmospheric Mercury: Global Constraints from Observations. Journal of geophysical research 2007, 112, D02308.

(32). Guttikunda SK; Jawahar P Atmospheric Emissions and Pollution from the Coal-Fired Thermal Power Plants in India. Atmospheric Environment 2014, 92, 449–460.

(33). Duan L; Wang X; Wang D; Duan Y; Cheng N; Xiu G Atmospheric Mercury Speciation in Shanghai, China. Science of The Total Environment 2017, 578, 460–468. [PubMed: 27856056]

(34). Han D; Zhang J; Hu Z; Ma Y; Duan Y; Han Y; Chen X; Zhou Y; Cheng J; Wang W Particulate Mercury in Ambient Air in Shanghai, China: Size-Specific Distribution, Gas–Particle Partitioning, and Association with Carbonaceous Composition. Environmental Pollution 2018, 238, 543–553. [PubMed: 29605614]

(35). Chen X; Balasubramanian R; Zhu Q; Behera SN; Bo D; Huang X; Xie H; Cheng J Characteristics of Atmospheric Particulate Mercury in Size-Fractionated Particles during Haze Days in Shanghai. Atmospheric Environment 2016, 131, 400–408.

(36). Lehodey P; Senina I; Nicol S; Hampton J Modelling the Impact of Climate Change on South Pacific Albacore Tuna. Deep Sea Research Part II: Topical Studies in Oceanography 2015, 113, 246–259.

(37). Sunderland EM; Li M; Bullard K Decadal Changes in the Edible Supply of Seafood and Methylmercury Exposure in the United States. Environ. Health Perspect 2018, 126 (1), 017006. [PubMed: 29342451]

(38). Knightes CD Development and Test Application of a Screening-Level Mercury Fate Model and Tool for Evaluating Wildlife Exposure Risk for Surface Waters with Mercury- Contaminated Sediments (SERAFM). Environmental Modelling & Software 2008, 23 (4), 495–510.

(39). Knightes CD; Sunderland EM; Barber MC; Johnston JM; Ambrose RB Application of Ecosystem-Scale Fate and Bioaccumulation Models to Predict Fish Mercury Response Times to Changes in Atmospheric Deposition. Environmental Toxicology and Chemistry 2009, 28 (4), 881–893. [PubMed: 19391686]

(40). Brown S; Saito L; Knightes C; Gustin M Calibration and Evaluation of a Mercury Model for a Western Stream and Constructed Wetland. Water Air Soil Pollut 2007, 182 (1–4), 275–290.

(41). Selin NE; Sunderland EM; Knightes CD; Mason RP Sources of Mercury Exposure for US Seafood Consumers: Implications for Policy. Environmental health perspectives 2010, 118 (1), 137–143. [PubMed: 20056570]

(42). Hong Y-S; Rifkin E; Bouwer EJ Modeling Mercury Distribution in the Sarasota Bay Ecosystem Using SERAFM and Stable Isotope Ratios of Nitrogen (Δ15N) in Biota. Environmental Engineering Science 2014, 31 (3), 135–147.

(43). Hope Bruce K; Louch Jeff. Pre-anthropocene Mercury Residues in North American Freshwater Fish. Integrated Environmental Assessment and Management 2013, 10 (2), 299–308.

(44). Hope BK Efficacy of Translators for Establishing Mercury Total Maximum Daily Loads. Human and Ecological Risk Assessment: An International Journal 2011, 17 (6), 1263–1278.

(45). Gidley PT; Kreitinger JP; Zakikhani M; Suedel BC Methylmercury Screening Models for Surface Water Habitat Restoration: A Case Study in Duluth-Superior Harbor; ERDC/EL TR-17–19; ERDC-EL Vicksburg United States, ERDC-EL Vicksburg United States, 2017.

(46). Zhu S; Žhang Z; Zagar D Mercury Transport and Fate Models in Aquatic Systems: A Review and Synthesis. Science of The Total Environment 2018, 639, 538–549. [PubMed: 29800847]

(47). Hendricks AN A Model to Predict Concentrations and Uncertainty for Mercury Species in Lakes Open Access Master's Thesis, Michigan Technological University: http://digitalcommons.mtu.edu/etdr/585, 2018.

(48). Perlinger JA; Urban NR; Giang A; Selin NE; Hendricks AN; Zhang H; Kumar A; Wu S; Gagnon VS; Gorman HS; Norman E Responses of Deposition and Bioaccumulation in the Great Lakes Region to Policy and Other Large-Scale Drivers of Mercury Emissions. Environmental Science: Processes & Impacts 2018, 20 (1), 195–209. [PubMed: 29360116]

(49). Håkanson L The Derivation and Use of a Dynamic Model for Mercury in Lake Fish Based on a Static (Regression) Model. Water, Air, & Soil Pollution 2000, 124 (3–4), 301–317.

(50). Barber MC Dietary Uptake Models Used for Modeling the Bioaccumulation of Organic Contaminants in Fish. Environmental Toxicology and Chemistry 2008, 27 (4), 755–777. [PubMed: 18333698]

(51). Thevenon F; Graham ND; Chiaradia M; Arpagaus P; Wildi W; Poté J Local to Regional Scale Industrial Heavy Metal Pollution Recorded in Sediments of Large Freshwater Lakes in Central Europe (Lakes Geneva and Lucerne) over the Last Centuries. Science of the Total Environment 2011, Complete (412–413), 239–247.

(52). Glass GE; Sorensen JA; Schmidt KW; Rapp GR New Source Identification of Mercury Contamination in the Great Lakes. Environ. Sci. Technol 1990, 24 (7), 1059–1069.

(53). Kuhnlein HV; Chan HM Environment and Contaminants in Traditional Food Systems of Northern Indigenous Peoples. Annual Review of Nutrition 2000, 20 (1), 595–626.

(54). Eagles-Smith CA; Silbergeld EK; Basu N; Bustamante P; Diaz-Barriga F; Hopkins WA; Kidd KA; Nyland JF Modulators of Mercury Risk to Wildlife and Humans in the Context of Rapid Global Change. Ambio 2018, 47 (2), 170–197. [PubMed: 29388128]

(55). Krabbenhoft DP; Sunderland EM Global Change and Mercury. Science 2013, 341 (6153), 1457–1458. [PubMed: 24072910]

(56). Ahonen SA; Hayden B; Leppänen JJ; Kahilainen KK Climate and Productivity Affect Total Mercury Concentration and Bioaccumulation Rate of Fish along a Spatial Gradient of Subarctic Lakes. Science of The Total Environment 2018, 637–638, 1586–1596.

(57). Giang A; Selin NE Benefits of Mercury Controls for the United States. PNAS 2016, 113 (2), 286–291. [PubMed: 26712021]

(58). Muntean M; Janssens-Maenhout G; Song S; Selin NE; Olivier JGJ; Guizzardi D; Maas R; Dentener F Trend Analysis from 1970 to 2008 and Model Evaluation of EDGARv4 Global Gridded Anthropogenic Mercury Emissions. Science of The Total Environment 2014, 494–495, 337–350.

(59). Muntean M; Janssens-Maenhout G; Song S; Giang A; Selin NE; Zhong H; Zhao Y; Olivier JGJ; Guizzardi D; Crippa M; Schaaf E; Dentener F Evaluating EDGARv4.Tox2 Speciated Mercury Emissions Ex-Post Scenarios and Their Impacts on Modelled Global and Regional Wet Deposition Patterns. Atmospheric Environment 2018, 184, 56–68.

(60). US EPA. 2011 National Emissions Inventory (NEI) Data https://www.epa.gov/air-emissions-inventories/2011-national-emissions-inventory-nei-data (accessed May 8, 2018).

(61). Smith CM; Trip LJ Mercury Policy and Science in Northeastern North America: The Mercury Action Plan of the New England Governors and Eastern Canadian Premiers. Ecotoxicology 2005, 14 (1–2), 19–35. [PubMed: 15931956]

(62). Stein AF; Draxler RR; Rolph GD; Stunder BJB; Cohen MD; Ngan F NOAA's HYSPLIT Atmospheric Transport and Dispersion Modeling System. Bull. Amer. Meteor. Soc 2015, 96 (12), 2059–2077.

(63). Sunderland EM; Cohen MD; Selin NE; Chmura GL Reconciling Models and Measurements to Assess Trends in Atmospheric Mercury Deposition. Environmental Pollution 2008, 156, 526–535. [PubMed: 18299164]

(64). French JP Autoimage: Multiple Heat Maps for Projected Coordinates. R J 2017, 9 (1), 284–297. [PubMed: 29147579]

(65). O'Neill C Mercury, Risk, and Justice; SSRN Scholarly Paper ID 1004769; Social Science Research Network: Rochester, NY, 2007.

(66). US EPA. Wabanaki Traditional Cultural Lifeways Exposure Scenario https://www.epa.gov/tribal/wabanaki-traditional-cultural-lifeways-exposure-scenario (accessed May 8, 2018).

(67). Xue J; Zartarian V; Mintz B; Weber M; Bailey K; Geller A Modeling Tribal Exposures to Methyl Mercury from Fish Consumption. Science of The Total Environment 2015, 533, 102–109. [PubMed: 26151654]

(68). Ranco DJ; O'Neill CA; Donatuto J; Harper BL Environmental Justice, American Indians and the Cultural Dilemma: Developing Environmental Management for Tribal Health and Well-Being. Environmental Justice 2011, 4 (4), 221–230.

(69). US EPA. Region 1 Fish Tissue Contamination QA Plan | Regional Environmental Monitoring and Assessment Program | US EPA https://archive.epa.gov/emap/archive-emap/web/html/reg1_rpt.html (accessed May 8, 2018).

(70). US EPA. Water Quality Criteria: Notice of Availability of Water Quality Criterion for the Protection of Human Health: Methylmercury https://www.federalregister.gov/documents/2001/01/08/01-217/water-quality-criteria-notice-of-availability-of-water-quality-criterion-for-the-protection-of-human (accessed May 8, 2018).

(71). Gagnon V; Gorman H; Norman E Power and Politics in Research Design and Practice: Opening up Space for Social Equity in Interdisciplinary, Multi-Jurisdictional and Community-Based Research. Gateways: International Journal of Community Research and Engagement 2017, 10 (0), 164–184.

(72). Hutcheson MS; Smith CM; Rose J; Batdorf C; Pancorbo O; West CR; Strube J; Francis C Temporal and Spatial Trends in Freshwater Fish Tissue Mercury Concentrations Associated with Mercury Emissions Reductions. Environ. Sci. Technol 2014, 48 (4), 2193–2202. [PubMed: 24494622]

(73). Brigham ME; Sandheinrich MB; Gay DA; Maki RP; Krabbenhoft DP; Wiener JG Lacustrine Responses to Decreasing Wet Mercury Deposition Rates—Results from a Case Study in Northern Minnesota. Environ. Sci. Technol 2014, 48 (11), 6115–6123. [PubMed: 24837007]

(74). Zhou H; Zhou C; Lynam MM; Dvonch JT; Barres JA; Hopke PK; Cohen M; Holsen TM Atmospheric Mercury Temporal Trends in the Northeastern United States from 1992 to 2014: Are Measured Concentrations Responding to Decreasing Regional Emissions? Environ. Sci. Technol. Lett 2017, 4 (3), 91–97.

(75). US Fish and Wildlife service. Contaminant Assessment of White Suckers from Eight Rivers in the Gulf of Maine Distinct Population Segment for Atlantic Salmon; FY07-MEFO-1-EC; Maine Field Office, 2007; p 44.

(76). US Fish and Wildlife service. First Micmac Fish Harvest https://usfwsnortheast.wordpress.com/2017/06/28/first-micmac-fish-harvest/ (accessed May 8, 2018).

(77). Outridge PM; Mason RP; Wang F; Guerrero S; Heimburger-Boavida LE Updated Global and Oceanic Mercury Budgets for the United Nations Global Mercury Assessment 2018. Environ. Sci. Technol 2018, 52 (20), 11466–11477.

(78). Engstrom DR; Fitzgerald WF; Cooke CA; Lamborg CH; Drevnick PE; Swain EB; Balogh SJ; Balcom PH Atmospheric Hg Emissions from Preindustrial Gold and Silver Extraction in the Americas: A Reevaluation from Lake-Sediment Archives. Environ. Sci. Technol 2014, 48 (12), 6533–6543. [PubMed: 24819278]

(79). Amos HM; Sonke JE; Obrist D; Robins N; Hagan N; Horowitz HM; Mason RP; Witt M; Hedgecock IM; Corbitt ES; Sunderland EM Observational and Modeling Constraints on Global Anthropogenic Enrichment of Mercury. Environ. Sci. Technol 2015, 49 (7), 4036–4047. [PubMed: 25750991]

(80). Beal S; Osterberg EC; Zdanowicz C; Fisher D An Ice Core Perspective on Mercury Pollution during the Past 600 Years. Environmental Science and Technology 2015, 49 (13), 7641–7647. [PubMed: 26011603]

(81). Zhang Y; Jaeglé L; Thompson L; Streets DG Six Centuries of Changing Oceanic Mercury. Global Biogeochemical Cycles 2014, 28 (11), 1251–1261.

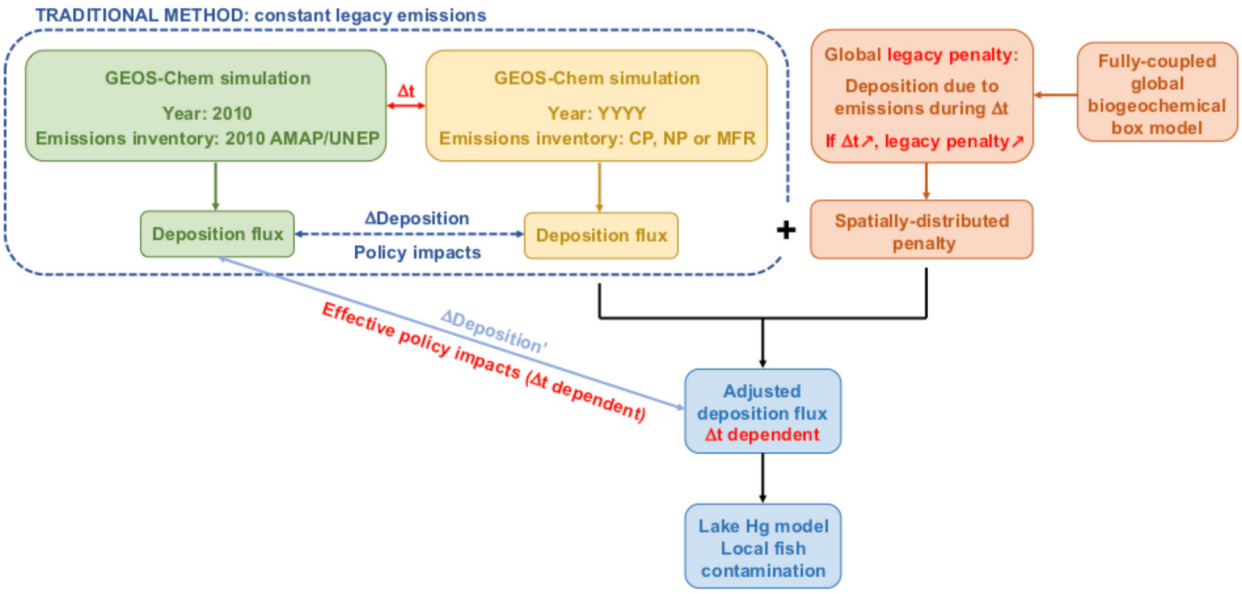

Figure 1:

Conceptual framework. Due to a challenging parameterization, chemical transport models (CTMs, GEOS-Chem in this study) traditionally hold legacy emissions constant at present-day (2010) levels when making future projections. The latter thus only reflect changes in direct anthropogenic emissions. Using a fully-coupled seven-reservoir global biogeochemical cycle model[11,16] we account for future legacy emissions as a result of both past and future emissions by adjusting GEOS-Chem outputs. The effective policy impacts in terms of local Hg deposition are then dependent on policy delay. The adjusted deposition flux is then used as input to a lake Hg model to evaluate the response of fish contamination to delayed action. Current Policy (CP), New Policy (NP) and Maximum Feasible Reduction (MFR) refer to future global emissions scenarios developed by Pacyna et al.[9].

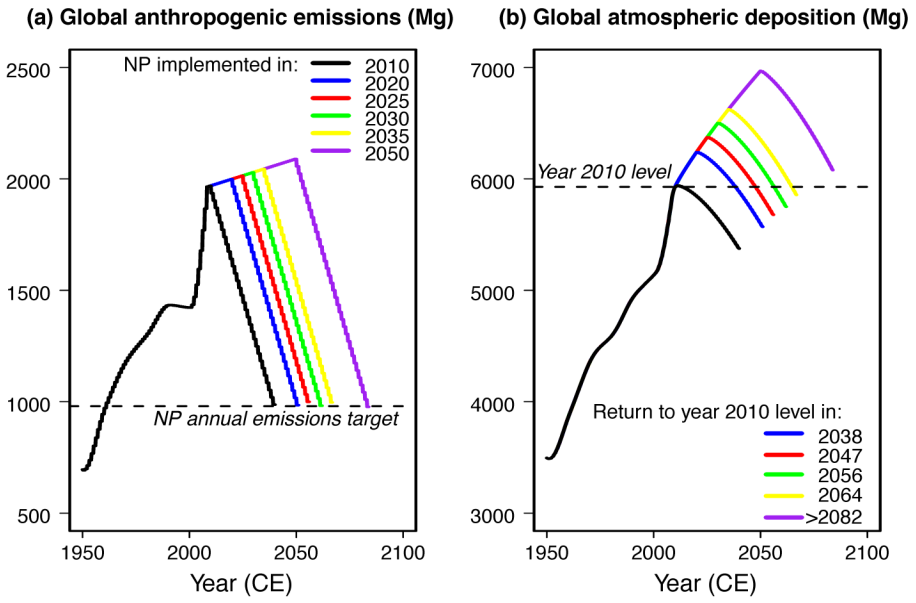

Figure 2:

(a) Global primary anthropogenic emissions of Hg to the atmosphere (in Mg). A New Policy (NP) is implemented in 2010 (black), 2020 (blue), 2025 (red), 2030 (green), 2035 (yellow) or 2050 (purple). The NP annual emissions target[9] is reached at a rate of −32.7 Mg yr^{-1} even in case of delayed global action. **(b)** Global atmospheric Hg deposition to ecosystems (in Mg). Each 5-year delay in implementing NP delays by additional extra ca. 4 years the return of Hg deposition to its year 2010 level (chosen for illustrative purposes) due to legacy emissions.

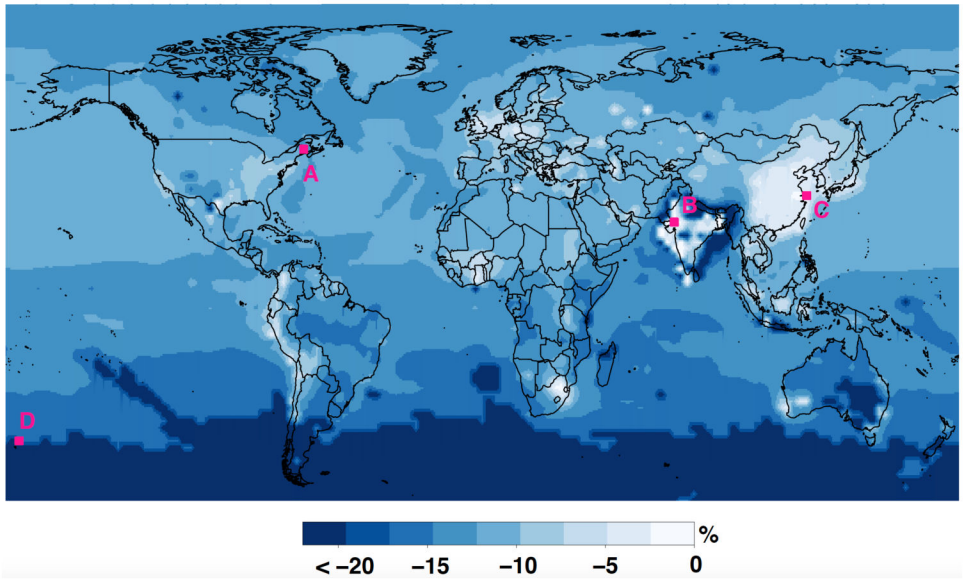

Figure 3:

Mean percent change in policy impacts due to a near-term (2020-2035) 5-year delayed implementation of a New Policy (NP) scenario. Results are discussed at selected sites with varying impact from emissions sources, focusing on A) tribal areas of Eastern Maine, USA, B) Ahmedabad, India, C) Shanghai, China, and D) an area of the Southern Pacific known for albacore tuna fisheries. This Figure was made using the R package autoimage[64].

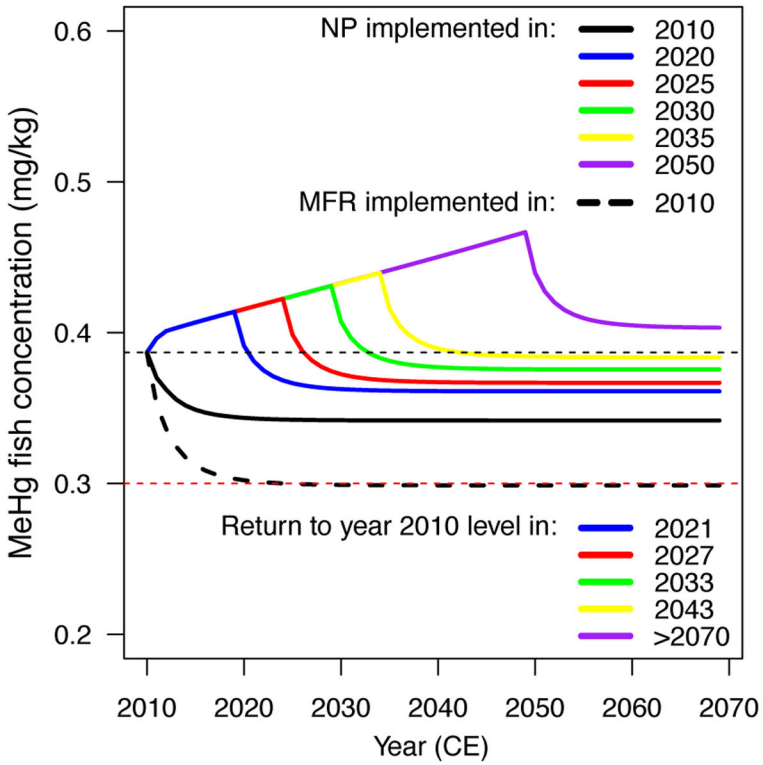

Figure 4:

Median response of Eastern Maine (USA) lacustrine predatory fish contamination to delayed implementation of a New Policy (NP) or Maximum Feasible Reduction (MFR) scenario. Black dashed line: year 2010 MeHg concentration. Red dashed line: U.S. EPA reference dose for MeHg (0.3 mg kg^{-1}).

Table 1:

Simulations performed with the chemical transport model (CTM) GEOS-Chem and the seven-reservoir global biogeochemical cycle (GBC) model[11,16]. Current Policy (CP), New Policy (NP), and Maximum Feasible Reduction (MFR) refer to future global emissions scenarios developed by Pacyna et al.[9]. A number of simulations listed here were performed to check the robustness of the method (see S.I. Section 1.1).

Simulation	CTM Meteorological year simulated: 2010*	Global biogeochemical cycle (GBC) model Years simulated: 2000 BCE-2100 CE
BASE	2010 AMAP/UNEP inventory[17] and emissions controls[18] **.	Street et al.[19] from 2000 BCE to 2008 CE. CP from 2009 onward.
PRE-2010 LEGACY	Primary anthropogenic emissions zeroed out.	Primary anthropogenic emissions completely eliminated as of 2010.
FUTURE	Future (CP, NP or MFR) emissions inventories[9].	NP or MFR implemented in YYYY = 2010, 2020, 2025, 2030, 2035 or 2050.
PRE-YYYY LEGACY	Same as PRE-2010 LEGACY since 2010-YYYY emissions are not taken into account	Primary anthropogenic emissions completely eliminated as of: YYYY = 2020, 2025, 2030, 2035 or 2050.

*The model was run for meteorological years 2007-2010, with the first three years used as the initialization period. We used consistent 2007-2010 meteorology for present and future runs to isolate the effect of emissions.

**In order to evaluate present-day model outputs against observations and account for inter-annual variability, this simulation was also performed for meteorological years 2009-2015 following a three-year spin-up.

Table 2:

Policy impact on local Hg deposition ($\Delta\mu g/m^2/yr$, percent in parentheses) assuming an immediate implementation and no legacy penalty (traditional method). Policy impact is calculated as the difference in deposition between FUTURE and BASE simulations. The following columns give the percent change in policy impact depending on year of implementation, i.e., length of the delay. The percent change in policy impact is calculated according to Equation (1). The mean percent change in policy impact is the average percent change due to a near-term (2020-2035) 5-year delay, calculated according to Equation (2). New Policy (NP) and Maximum Feasible Reduction (MFR) refer to future global emissions scenarios developed by Pacyna et al.[9].

	Policy impact in $\Delta\mu g/m^2/yr$ under traditional method (% change vs. present)	**Percent change in policy impact (%)**					
Year of implementation	***Traditional method***	***2020***	***2025***	***2030***	***2035***	***2050***	***mean***
Global average							
NP	−1.4 (−13.6%)	−33.6	−48.5	−62.7	−76.2	−114.1	−14.2
MFR	−2.5 (−23.8%)	−19.1	−27.5	−35.5	−43.2	−64.6	−8.0
Global legacy penalty (Mg)	0.0	272	392	506	615	921	114.5
Maine, USA (A)							
NP	−2.9 (−15.3%)	−29.5	−42.6	−55.0	−66.9	−100.0	−12.5
MFR	−4.9 (−25.8%)	−17.5	−25.3	−32.7	−39.7	−59.5	−7.4
Ahmedabad, India (B)							
NP	+4.2 (+25.9%)	−12.7	−18.4	−23.7	−28.9	−43.2	−5.4
MFR	−6.3 (−38.4%)	−8.6	−12.4	−16.0	−19.5	−29.2	−3.6
Shanghai, China (C)							
NP	−6.3 (−55.1%)	−2.7	−3.9	−5.0	−6.1	−9.1	−1.1
MFR	−7.8 (−68.3%)	−2.2	−3.1	−4.1	−4.9	−7.4	−0.9
South Pacific (D)							
NP	−1.7 (−12.9%)	−38.3	−55.3	−71.4	−86.9	−130.1	−16.2
MFR	−3.0 (−22.1%)	−22.8	−32.8	−42.4	−51.6	−77.2	−9.6